Switching studies for the Horns Rev 2 wind farm main cable

Jensen, Christian Flytkjær; Faria da Silva, Filipe; Bak, Claus Leth; Wiechowski, W.

Published in:
Proceedings of the International Conference on Power Systems Transients, IPST 2011

Publication date:
2011

Document Version
Publisher's PDF, also known as Version of record

Switching studies for the Horns Rev 2 wind farm main cable

C.F. Jensen, F. Faria da Silva , C.L. Bak, and W. Wiechowski

***Abstract*—This article proposes a method of constructing a PSCAD model suitable for switching studies in a system containing long HVAC cables. The transmission network connection to the 215 MW offshore wind farm Horns Rev 2 is used as a case study. The connection to Horns Rev 2 consists of two land cable sections with a total length of 57.7 km and a 42 km long submarine cable. The submarine cable is a three phase type of cable, and three single conductor cables are used for the land cable system. Methods of recalculating the physical cable parameters given in the data sheet to parameters suitable for the cable model used in PSCAD are presented. Results obtained using the model are compared to full scale measurement of the energization of the system, and good agreement is found. The influence of different simulation parameters are examined; amongst them the modelling of the screen, the relative permittivity, and the use of different cable models.**

***Index Terms* – Electromagnetic Transients, Cable models, Overvoltages, PSCAD.**

I. Introduction

In order to reduce visual pollution, the Danish government has decided to replace the existing 132/150 kV overhead line system with HVAC power cables [4]. This introduces new difficulties as a high voltage cable possesses 20-50 times higher capacitance per unit length compared to an equivalent overhead line [11, p. 157]. Because the capacitance is high, the production of reactive power is also high. The additional flow of reactive power leads to a reduction of the active power transfer capability and to additional losses. Moreover, steady state voltage rises can occur due to the capacitive reactive currents flowing through transmission lines and transformers. To compensate for the additional reactive power production, shunt reactors are installed strategic places in the power grid. These reactors consume reactive power and thereby reduces the steady state overvoltages. When the reactors are used along cables, series and parallel resonance circuits are formed and they can drastically change the dynamic behaviour of the system. Because of the resonant circuit behaviour, overvoltages and overcurrents can occur in the system. These overvoltages and overcurrents can damage system components if the overvoltages or overcurrents exceed a critical value determined by the components. To limit the destructive effect of such overvoltages, surge arresters are installed. These components add to the total system cost, and should therefore be selected to match the system. To be able to properly select the surge arrestors, simulations of worst case switching scenarios are performed. As these simulations are the ground foundation for selecting the arresters, it is of great importance that the simulation results can be trusted. Even with the most advanced cable models the simulation results are no better than the input parameters given. With the current versions of PSCAD, no accurate representation of the cables physical structure is available in the models. Therefore several methods for recalculating the necessary parameters have been developed [3]. The correct use of these methods is presented in this article where a model of the electrical connection to the Horns Rev 2 offshore wind farm in the simulation program PSCAD is constructed. The model is verified against full scale measurement, and the importance of different simulation parameters is identified.

The cable connection from the 400/150 kV substation Endrup to Horns Rev 2 is shown in Fig. 1.

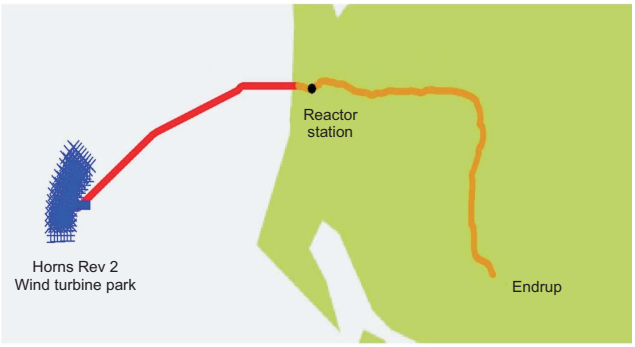

Figure 1. Cable connection between station Endrup and wind farm Horns Rev 2 in Denmark [5].

II. System description

Horns Rev 2 is a 215 MW wind farm located 30 km outside the west coast of Denmark. The cable connection consists of two land cable sections with a combined length of 57.7 km and a 42 km submarine cable. To compensate for the reactive power production of the cables a 80 MVAr shunt reactor is installed 2.3 km from the connection point between the land and submarine cable. Additionally two reactors of 40 and 80 MVAr are installed in substation Endrup. Finally a 400 MVA autotransformer is used to connect Horns Rev 2 to the 400 kV transmission grid. A single line diagram of the system is presented in Fig. 2.

The land cable connection consist of three single phase aluminium conductor cables each having a cross section of

C.F. Jensen is with Energinet.dk (e-mail of corresponding author: cfj@energinet.dk)

F. Faria da Silva is with Energinet.dk (e-mail of corresponding author: fms@energinet.dk)

C.L. Bak is with the Department of Energy Technology, Aalborg University (e-mail of corresponding author: clb@et.aau.dk)

W. Wiechowski is with WTW Power Solutions (e-mail of corresponding author: wtw@wtwps.com)

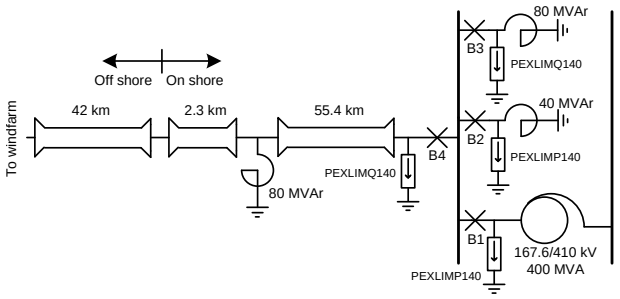

Figure 2. Single line representation of station Endrup and the Horns Rev 2 wind farm on shore connection.

1200 mm^2 and a rated voltage of 165 kV. The three cables are laid in tight trefoil formation and the screens are cross bonded using 11 major sections. The lengths of the minor sections varies from 0.586 km to 1.823 km. The cable is shown in Fig. 3.

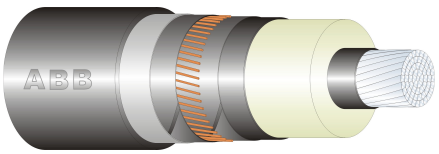

Figure 3. Physical layout of single conductor ABB land cable [1].

The diameter of a single screen copper wire is 1.11 mm and the longitudinal water barrier is made of aluminium. The parameters given by the manufacture are presented in Table I.

Table I
ABB LAND CABLE PARAMETERS.

Parameter	Value
Conductor aluminium [mm^2]	1200
Conductor outer diameter [mm]	41.5
Conductor screen thickness [mm]	1.5
Insulation diameter [mm]	79
Insulation screen thickness [mm]	1.0
Longitudinal water barrier [mm]	0.6
Copper wire screen cross section [mm^2]	95
Longitudinal water barrier thickness [mm]	0.6
Radial water barrier thickness [mm]	0.2
Outer cover diameter [mm]	95

The submarine cable is a three core 640 mm^2 copper cable produced by Nexans with a voltage rating of 165 kV. In Fig. 4 the layout of the three phase submarine cable is shown.

The cable parameters are shown is Table II.

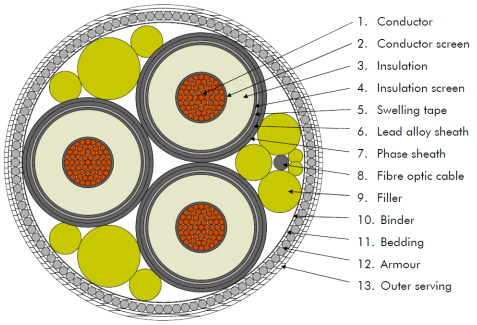

Figure 4. Layout of the three phase submarine cable [10].

Table II
NEXANS SUBMARINE CABLE PARAMETER.

Parameter	Value
Conductor copper [mm^2]	640
Conductor outer diameter [mm]	30.5
Conductor screen thickness [mm]	1.5
Insulation diameter [mm]	69.5
Insulation screen diameter [mm]	75.5
Lead screen outer diameter [mm^2]	80.3
Longitudinal water barrier thickness [mm]	0.6
Phase screen diameter [mm]	84.9
Outer cover diameter [mm]	95

III. SIMULATIONS MODEL SETUP

One of the most advanced electromagnetic transient software available today for the simulation of power systems containing long HVAC cables is EMTDC/PSCAD. EMTDC/PSCAD has the most accurate cable model implemented - the frequency dependent phase model [9]. Parameters related to geometry are given as input to the model and from these the electrical parameters are calculated. The geometrical layout of the cable model implemented in PSCAD is seen in Fig. 5.

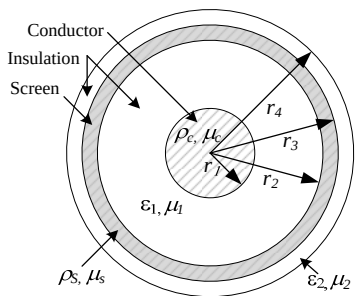

Figure 5. General representation of cable model implemented in PSCAD.

Comparing Fig. 3 and 4 to the layout shown in Fig. 5, it can be seen that there are several differences in the complexity of the configurations. All layers in the cable model are represented as solid layers of one material only. In a real cable the conductor is often stranded in order to ensure flexibility of the cable. The semiconducting screens are not included in the model at all. The screen is often made of wires with a cross section smaller than the one represented by the solid screen. It is also noticed that two different materials are used for the

screen of the land cable (Cu and Al). All this requires that the cable parameters are recalculated to fit the PSCAD model. Methods for doing this are presented in the following sections.

A. The inner conductor

As it is the case for many types of HVAC power cables, segmented conductors are used for both the land and submarine cable. This is, as mentioned, not possible to model in PSCAD. The effective resistivity of the conductor must therefore be increased. This can be done by multiplying the resistivity with the relationship between the physical area used by the conductor and the effective cross section [3].

$$\rho' = \rho \, \frac{r_1^2 \cdot \pi}{A} \qquad [\Omega\mathrm{m}] \tag{1}$$

Where A is the effective cross section of the conductor and r_1 is the radius of the inner phase conductor.

B. The relative permittivity

The semiconducting layers are, as mentioned, not included in the current cable models. They can be taken into account by increasing the relative permittivity of the insulation material [3], [7, p. 5].
The capacitance from the conductor to the screen can, neglecting the resistive effect of the layers, be represented as a series coupling of the capacitance across the first semiconducting layer, the capacitance across the insulation material and the capacitance across the second semiconducting layer [2]. Because the capacitance of the insulation material is many times smaller than the capacitance of the semiconducting layers, the equivalent capacitance can be set equal to that of the insulation material without introducing significant errors.

The capacitance of a cable without semiconducting layers is calculated as:

$$C = \epsilon_i \, \frac{2\pi l}{\ln\left(\frac{b}{a}\right)} \qquad [\mathrm{F}] \tag{2}$$

where b and a are the outer and inner radius of the insulation respectively. ϵ_i is the permittivity of the insulating material

When calculating the capacitance taking into account the semiconducting layers, Equation 2 is rewritten to:

$$C = \epsilon' \, \frac{2\pi l}{\ln(\frac{r_2}{r_1})} \qquad [\mathrm{F}] \tag{3}$$

where r_1 and r_2 are defined in Fig. 5.

Equation 2 and 3 are set equal and the corrected permittivity is found. The result is shown in Equation 4.

$$\epsilon' = \epsilon_i \, \frac{\ln(\frac{r_2}{r_1})}{\ln\left(\frac{b}{a}\right)} \qquad [-] \tag{4}$$

C. The outer screen

The outer screen can be constructed in many different ways. This makes the use of a general method difficult. In [8] it is proposed to *'replace the sheath with a tubular conductor having a cross section area equal to the total wire area'*. This is shown in Equation 5.

$$r_3 = \sqrt{\frac{A_s}{\pi} + r_2^2} \qquad [\mathrm{m}] \tag{5}$$

where A_s is the cross section of the screen, and r_2 and r_3 are defined in Fig. 5. Another method proposed by this author, for screens made of single wires, is to increase the resistivity of the wire material as it was done for the conductor. This is done by multiplying the screen resistivity by the relationship between the cross section area of the screen layer and the effective cross section of the screen layer. This is shown in Equation 6.

$$\rho'_{s,cu} = \rho_{s,Cu} \frac{\pi(r_3^2 - r_{2,sh}^2)}{A_s} \qquad [\Omega\mathrm{m}] \tag{6}$$

where r_3 is the outer radius of the screen, $r_{2,sh}$ is the inner layer of the insulation plus the semiconducting screen layer and A_s is the effective area of the screen.

The outer screen of the land cable consists of two different materials - copper and aluminium. This can be taken into account by finding an equivalent resistivity on the basis on the cross sections of the two layers after using Equation 6 for the copper wire screen. The equation for calculating the equivalent resistivity is shown in Equation 7.

$$\rho_{eq} = \rho'_{s,Cu} \frac{A_{Cu}}{A_{Cu} + A_{Al}} + \rho_{al} \frac{A_{Al}}{A_{Cu} + A_{Al}} \qquad [\Omega\mathrm{m}] \tag{7}$$

where $\rho'_{s,Cu}$ is calculated using Equation 6.

Using the described methods the parameters for the land cable is found to be as shown in Table III.

Table III
PSCAD CABLE MODEL PARAMETERS FOR THE ABB LAND CABLE.

Parameter	Value
r_1	20.75 mm
r_2	40.5 mm
r_3	41.61 mm
r_4	47.5 mm
ϵ	2.74
ρ_c	3.156 $\cdot 10^{-8}$ Ω·m
ρ_s	3.65 $\cdot 10^{-8}$ Ω·m

The submarine cable is implemented using three single phase conductors disregarding the common outer screen. This can be done as each conductor has a separate metallic screen. The cable screen is grounded in both ends. The recalculated parameters for the submarine cable are seen in Table IV.

Table IV
PSCAD CABLE MODEL PARAMETERS FOR THE NEXANS SUBMARINE CABLE.

Parameter	Value
r_1	15.25 mm
r_2	37.75 mm
r_3	40.15 mm
r_4	42.45 mm
ϵ	2.857
ρ_c	1.999 $\cdot 10^{-8}$ Ω·m
ρ_s	2.2 $\cdot 10^{-8}$ Ω·m

The outer most layer of the single conductor is the semi-conducting phase screen. This can be modelled as a insulation layer with a relative permittivity of 1000 [3].

D. Screen cross bonding

The cross bonding of the land cable is implemented assuming an inductance of 1 μH/m for the cable used to interconnect the screens. The length of the cable connecting the cross bonded screens is approximately 1 m. For the land cable a cross bonding junction is implemented as shown in Fig. 6.

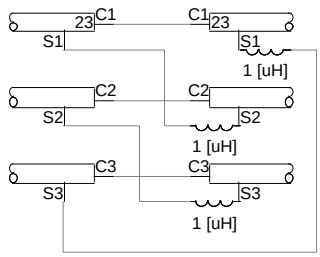

Figure 6. PSCAD implementation of cross bonding junction between two minor sections.

The grounding of the screens between two major sections is done in link boxes placed on the ground surface. The length from the screen to the box is approximately 10 m. The ground resistance is modeled as a simple 10 Ω resistance. This value is normally not know but is commonly between 10 and 20 Ω in Denmark. A junction between two major sections is modelled as shown in Fig. 7.

IV. CABLE ENERGIZATION

The cable is energized by closing breaker B4 (see Fig. 2) after all system voltages and currents are in steady state. The breaker uses synchronized switching at zero voltage crossing. This mechanism does not work perfectly and small deviations in the switching instance are included in the modelling of the breaker

The voltages at sending and receiving end are recorded as well as the current in the sending end for phase a and b. The phase to ground voltages at the breaker side of the station Endrup are simulated using the model described. The results for phase a, b and c are compared to full scale field test measurements done on the system and shown in Fig. 8.

The simulations and measurements are in good agreement. The steady state and peak voltages are given in Table V.

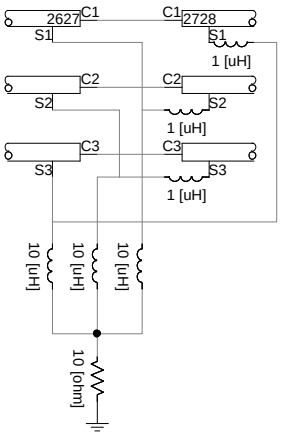

Figure 7. PSCAD implementation of grounded junction for cross bonding of the land cable.

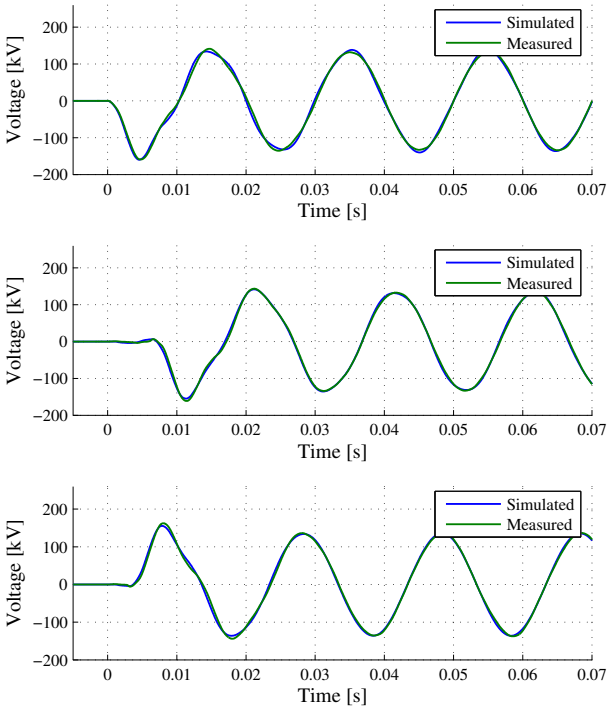

Figure 8. Simulated and measured phase to ground voltage at cable side of station Endrup for phase a, b and c (sending end).

Table V
STEADY STATE AND PEAK VOLTAGES AT THE SENDING END.

	Parameter	Unit	Simulated	Measured
Phase a	Steady state voltage	[kV]	96	95
	Peak voltage	[kV]	159	159
Phase b	Steady state voltage	[kV]	96	95
	Peak voltage	[kV]	158	161
Phase c	Steady state voltage	[kV]	96	95
	Peak voltage	[kV]	158	162

The voltages simulated and measured at the receiving end are shown in in Fig. 9.

The correlation is a bit lower for the voltages simulated at the receiving end of the cable. The voltage rise caused by the Ferranti effect is in the measurements 8% where in the

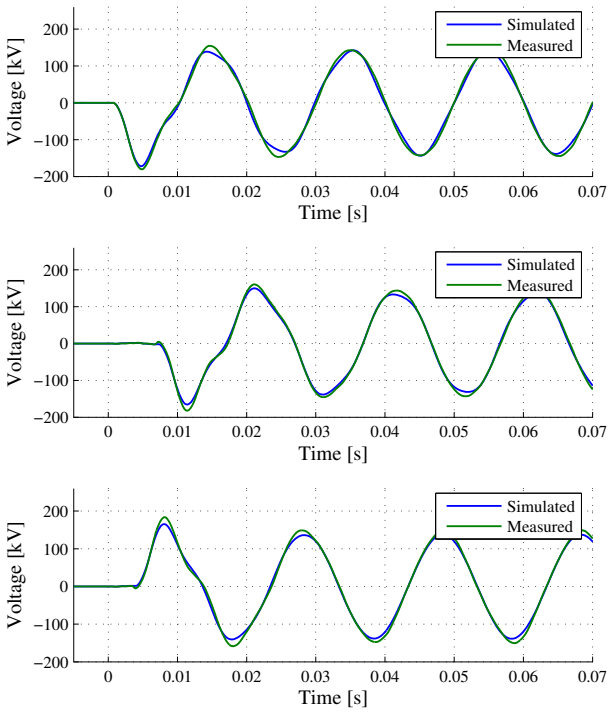

Figure 9. Simulated and measured phase to ground voltage at Horns Rev 2 for phase a, b and c (receiving end).

simulations only a voltage rise of 2.1 % is observed.

The steady state and peak voltages at the wind farm are given in Table VI.

Table VI
STEADY STATE AND PEAK VOLTAGES AT THE RECEIVING END.

	Parameter	Unit	Simulated	Measured
Phase a	Steady state voltage	[kV]	98	103
	Peak voltage	[kV]	172	180
Phase b	Steady state voltage	[kV]	98	103
	Peak voltage	[kV]	171	182
Phase c	Steady state voltage	[kV]	98	104
	Peak voltage	[kV]	172	183

The simulation and measurement of the current flowing into the land cable are shown in Fig. 10 for a low time resolution plot.

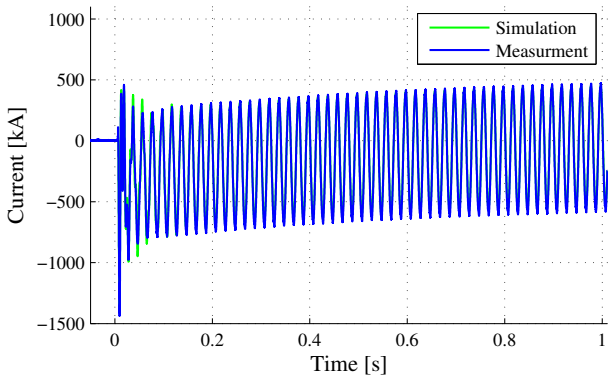

Figure 10. Simulated and measured low resolution current flowing in phase a measured at Endrup.

The DC-component of the current is at its maximum value because the switching was performed at zero voltage crossing [6]. The combined cable system produces approximately 200 MVAr. As the reactor between the two land cable sections is 80 MVAr, less than 50% of the total reactive power produced by the cable, no zero missing phenomena can occur at breaker B4 [6]. This is confirmed by both the simulation and measurement. The current in phase a using a high resolution plot is shown in Fig. 11.

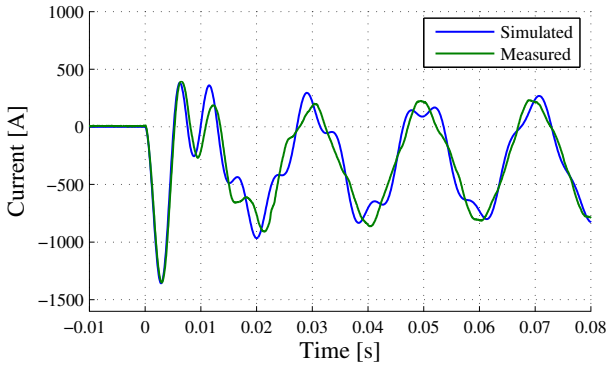

Figure 11. Simulated and measured high resolution current flowing in phase a measured at station Endrup.

The agreement between the simulated and measured current is high right after the instance of switching. The deviations after approx. 0.01 s are believed to be caused by different layer thickness between the three cables.

The current flowing into the land cable measured at station Endrup for phase b is simulated and measured as shown in Fig. 12.

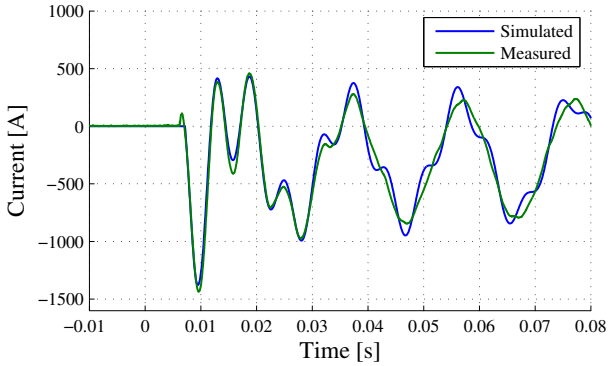

Figure 12. Simulated and measured high resolution current flowing in phase b measured at station Endrup.

The accuracy of the simulation for the current flowing in phase b is higher than for phase a. The results for phase a and b are given in Table VII

Table VII
STEADY STATE AND PEAK CURRENT FLOWING INTO LAND CABLE AT STATION ENDRUP FOR PHASE A AND B.

	Parameter	Unit	Simulated	Measured
Phase a	Steady state current	[A]	350	369
	Peak current	[A]	1357	1352
Phase b	Steady state current	[A]	351	369
	Peak current	[A]	1331	1436

Generally the simulation shows a lack of sufficient damping. There are several reasons for this. The reactor models, the transformer models and the representation of the short circuit impedance are not frequency dependent. Nor are the losses associated with the conductivity of the semiconducting layers or the dielectric losses taken into account because of their missing representation in the model [2].

V. THE EFFECT OF MODEL PARAMETERS

Wrong input parameters will lead to wrong simulation results. On the other hand, knowledge of how the simulation model can be optimized can lead to a considerable reduction in the time consumed when running the simulation and constructing the model. The effects of the most important parameters are examined in this section.

A. Relative permittivity

The relative permittivity of the insulating material was recalculated to take into account the effect of the semiconducting layers (see Equation 4). In this section the effects of not doing the recalculations but using the parameters directly from the manufactures are presented. The voltage and current simulated for an uncorrected and corrected relative permittivity are seen in Fig. 13 and 14.

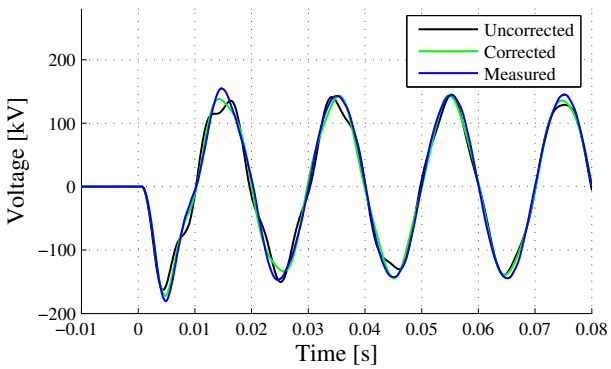

Figure 13. Measured and simulated phase to ground voltage at the sending end for a corrected and an uncorrected relative permittivity.

The correction of the relative permittivity shown to have a large effect on the results, and the recalculation is therefore important. The natural frequency of the system is a function of the capacitance which again is a function of the relative permittivity.

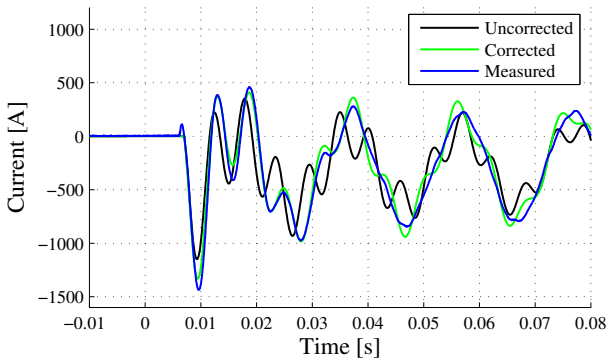

Figure 14. Measured and simulated current at the sending end for a corrected and an uncorrected relative permittivity.

B. Modelling the screen cross-bonding

The effect of correct representation of the screen cross bonding is examined in this section. Three different simulations are done; One with no cross bonding sections implemented, one with a single major section per cable, and one with all major sections implemented. The short land cable has already 1 major section where the long land cable section has 11. The short land cable is therefore represented correct for the two first cases described. The voltage and current measured and simulated at the sending end using all major sections, one major section, and no cross-bonding is shown in Fig. 15 and 16.

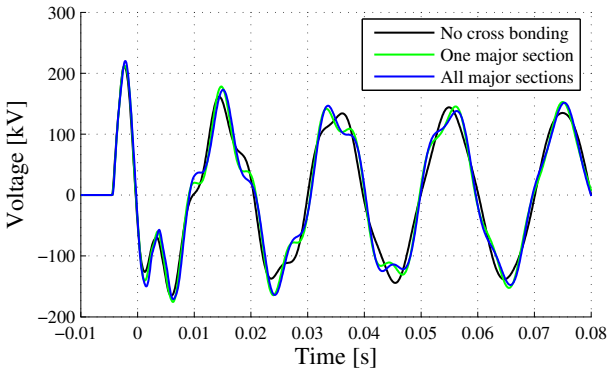

Figure 15. Measured and simulated phase to ground voltage at the sending end using all major sections, one major section, and no cross-bonding.

Because the wave forms are equal for the simulations with one and all major sections implemented, it can be concluded that it is not the reflections caused by the grounding of the screen at each third minor section that is important for low frequency switching studies. If this was the case, the results obtained with the two representations would deviate. What is important for the simulation is that the vector sum of the induced currents in the cable screens are equal in the two representations. This is roughly the case of both representations, and the model can therefore be greatly simplified by implementing only one major section per cable run. The simulation time for the simplified case is reduced to one fifth compared to a simulation with all major sections implemented.

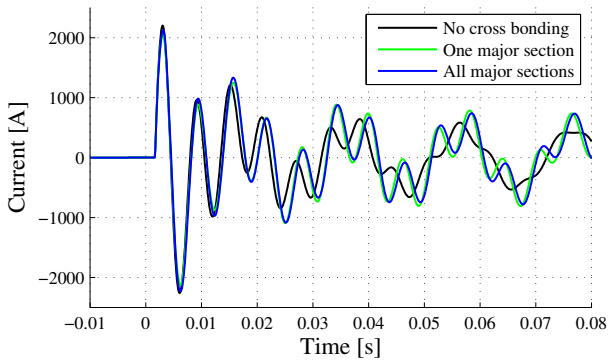

Figure 16. Measured and simulated current at the sending end for the land cable modeled using all major sections, one major section, and no cross-bonding.

C. Choice of cable model

The simulation time can be drastically reduced if a simpler model is used. The simulations are redone using Bergeron's model. The result is shown in Fig. 17 and 18.

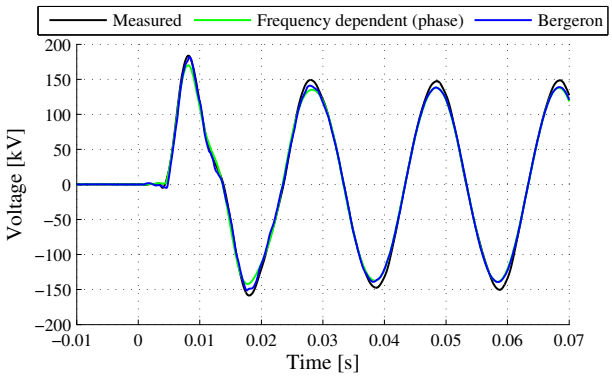

Figure 17. Measured and simulated phase to ground voltage at the receiving end using Bergeron's- and the frequency dependent phase mode.

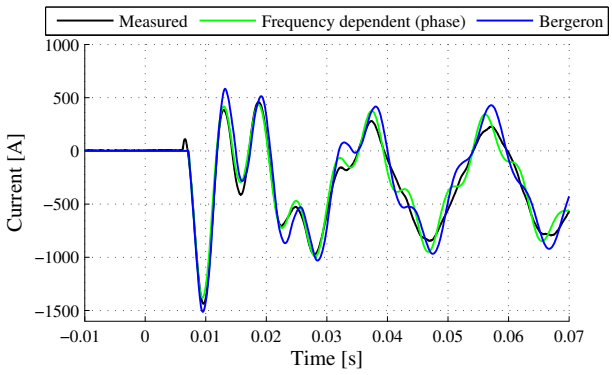

Figure 18. Measured and simulated sending end current using Bergeron's- and the frequency dependent phase model.

It can be seen from Fig. 17 and 18 that no final conclusion can be made regarding the performance of the two models. The dynamic behaviour is better represented by the frequency dependent phase model but the peak voltage is better predicted by Bergeron's model. Bergeron's model predicts the current peak larger than the measurements and the frequency dependent phase model. The conservative prediction by the frequency dependent phase model can be a problem, as the maximum current is a design parameter. The simulation time using Bergeron's model for the cable systems is reduced to one sixth compared to using the frequency dependent model where all major sections are implemented.

VI. Conclusion

In this paper a PSCAD model of the transmission network connection to the wind farm Horns Rev 2 was constructed. Methods for recalculating geometrical cable parameters from data screen values to values useable in the available PSCAD model were presented. The model was verified against full scale measurement and good agreement was found. It was shown that the presented method of taking into account the semiconducting layers by increasing the relative permittivity was important for the results. The modelling of the screen can be simplified in a system where cross bonding is used by using a single major section to represent the entire cable run. The dynamic behaviour is better predicted using the frequency dependent phase model compared to Bergeron's model. The maximum peak voltage is better predicted by Bergeron's model.

Acknowledgment

The authors would like to thank Unnur Stella Gudmundsdottir, Wojciech Tomasz Wiechowski, and Jakob Kessel for help regarding determination of parameters for system components and general discussions about cable models.

References

[1] ABB. *170 kV ABB cable design features*. ABB, first edition, 2009.
[2] Akihiro Ametani, Yukata Miyamoto, and Naoto Nagaoka. Semiconducting layer impedance and its effect on cable wave-propergation and transoents characteristics. *IEEE transactions on power delivery*, 19:1523 – 1531, 2004.
[3] Gustavsen B, Martinez, and D. J.A. Durbak. *Parameter determination for modeling system transients-Part II: Insulated cables*. IEEE Transactions on Power Delivery,, 2005.
[4] Energinet.dk. *Kabelhandlingsplan 132-150 kV*. Energinet.dk, 2009.
[5] Energinet.DK. *Transient studies of the Horns Rev 2 HVAC cable connection*. 2009.
[6] F. Faria da Silva, C.L. Bak, U.S. Guomundsdottir, W. Wiechowski, and M.R. Knardrupgard. Use of a pre-insertion resistor to minimize zero-missing phenomenon and switching overvoltages. *Power and Energy Society General Meeting*, 19:1–7, 2009.
[7] Unnur Stella Gudmundsdottir. *Comparison of PSCAD simulations and field test results*. Energinet.dk, 2008.
[8] Bjørn Gustavsen. Panel session on data for modeling system transients insulated cables. *Power Engineering Society Winter Meeting, IEEE*, 2:718 – 723, 2001.
[9] Manitoba HVDC Research Centre Inc. *Applications of PSCAD / EMTDC*. Manitoba HVDC Research Centre Inc.
[10] Nexans. *Technical Description of 170 kV Submarine Cable*. Nexans, first edition, 2009.
[11] S Vørts. *Elektriske fordelingsanlæg*. Polyteknisk forlag, 1990. ISBN - 87-502-0707-5.